

Organic & Biomolecular Chemistry

Accepted Manuscript



This is an *Accepted Manuscript*, which has been through the Royal Society of Chemistry peer review process and has been accepted for publication.

Accepted Manuscripts are published online shortly after acceptance, before technical editing, formatting and proof reading. Using this free service, authors can make their results available to the community, in citable form, before we publish the edited article. We will replace this *Accepted Manuscript* with the edited and formatted *Advance Article* as soon as it is available.

You can find more information about *Accepted Manuscripts* in the [Information for Authors](#).

Please note that technical editing may introduce minor changes to the text and/or graphics, which may alter content. The journal's standard [Terms & Conditions](#) and the [Ethical guidelines](#) still apply. In no event shall the Royal Society of Chemistry be held responsible for any errors or omissions in this *Accepted Manuscript* or any consequences arising from the use of any information it contains.

Cite this: DOI: 10.1039/c0xx00000x

www.rsc.org/xxxxxx

PAPER

N[1,3]-Sigmatropic Shift in the Benzidine Rearrangement: Experimental and Theoretical Investigation †

Shili Hou,[‡] Xinyao Li,[‡] and Jiaxi Xu*

Received (in XXX, XXX) Xth XXXXXXXXXX 20XX, Accepted Xth XXXXXXXXXX 20XX

DOI: 10.1039/b000000x

The N[1,3]-sigmatropic shift in the benzidine rearrangement has been studied in depth experimentally with the aid of the density functional theory (DFT) calculations. The designed substituted *N,N'*-diaryl hydrazines rearrange exclusively to the expected *o/p*-semidines and diphenylines. The intercrossing experiments support the intramolecular rearrangement process. Radical trapping experiments exclude the intermediacy of biradicals in the rearrangements. Computational results demonstrate that the *o*-semidine rearrangement involves a novel N[1,3]-sigmatropic shift and the *p*-semidine rearrangement proceeds tandem N[1,3]/N[1,3]-sigmatropic shifts, while the diphenylene rearrangement occurs through a cascade N[1,3]/[3,3]-sigmatropic shifts. The proposed mechanism involving the key N[1,3]-sigmatropic shift as the rate-limiting step is well consistent with reported kinetic isotope measurements. The combined methods provide the new insight into the formation mechanism of *o/p*-semidines and diphenylines in the benzidine rearrangement and propose the suprafacial symmetry allowed N[1,3]-sigmatropic shift with an inversion of the configuration in the migrating nitrogen atom unprecedentedly.

Introduction

The [1,3]-sigmatropic shift, as one of typical rearrangements in the thermal pericyclic rearrangements, is a powerful strategy for the construction of biologically active molecules in the synthetic organic chemistry.¹⁻⁵ The structure of the transition state and the configuration of the products in the [1,3]-sigmatropic shift have been predicted by the Woodward-Hoffmann selection rule through the suprafacial symmetry of the frontier molecular orbital approach with an inversion of the configuration in the migrating groups (Figure 1).⁶ Among them, C[1,3]-sigmatropic shift has been widely explored experimentally and theoretically,² while O/N[1,3]-sigmatropic shift was rarely reported. Recently, we have offered mechanistic insight of the O[1,3]-sigmatropic shift in the abnormal Claisen rearrangement.⁷ Now we are particularly interested in the N[1,3]-sigmatropic shift in some cases.

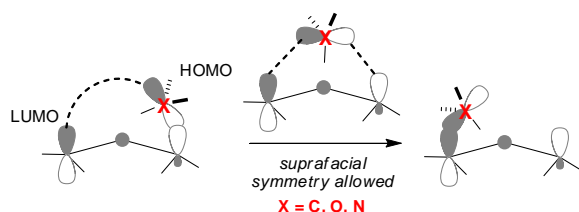
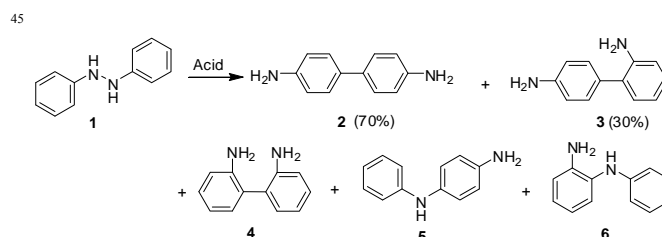


Fig. 1 Concerted [1,3]-sigmatropic shift with an inversion of the configuration in the migrating group.

Acid-catalyzed benzidine rearrangements have been studied extensively for more than 150 years,⁸ in which the parent *N,N'*-diphenyl hydrazine (**1**) gives *p*-benzidine (**2**, 70%) and diphenylene (**3**, 30%)^{9,10} as the main products and some other

secondary products such as *o*-benzidine (**4**), *p*-semidine (**5**), and *o*-semidine (**6**) (Scheme 1).¹¹ In some cases, *o*-benzidine, *p*-semidine, and *o*-semidine type products were obtained in considerable yields from certain substituted *N,N'*-diaryl hydrazines.



Scheme 1 Benzidine rearrangement of *N,N'*-diphenylhydrazine (**1**).

A large amount of work has been devoted to the mechanistic investigation of the benzidine rearrangements, where the controversies were concentrated on the polar transition state theory (one concerted step) and Dewar's π complex theory (two stepwise steps).¹² The question as to whether the rearrangement was stepwise or concerted mechanism was remained unresolved until measurements of heavy-atom kinetic isotope effects (KIEs) were performed by Shine and co-workers.¹³⁻¹⁵ A concerted [5,5]-sigmatropic shift was proposed on the basis of KIE results on nitrogen and carbon atoms for the formation of **2**. Furthermore, an inverse secondary deuterium isotopic effect for the disappearance of **1** supported the conclusion drawn from the nitrogen and carbon KIE results.^{13b,c} In contrast, the formation of diphenylene (**3**) was characterized *via* a substantial KIE for the N atom but with slight 2,2',6,6'-¹³C₄ KIE, in accord with an intramolecular and nonconcerted mechanism.^{13c} In addition, KIE

results for the formation of *o*-benzidines from *N,N'*-di(2-naphthyl)hydrazine and *N*-2-naphthyl-*N'*-phenylhydrazine were clearly indicative of a [3,3]-sigmatropic rearrangement.¹⁴ The nitrogen and carbon KIEs for the conversion of *N*-4-methoxyphenyl-*N'*-phenylhydrazine to the corresponding *p*-semidine and *o*-semidine were observed and the *p*-semidine rearrangement was assumed to be likely a concerted [1,5]-sigmatropic shift, whereas there was a slight 2,2',6,6'-¹³C₄ KIE for the *o*-semidine rearrangement.^{15a-c} Accordingly, the π -complex theory was ruled out by Shine's kinetic experiments, but it has been revived by recent calculations.^{16,17}

To date, the mechanisms for the formations of *p*-benzidines and *o*-benzidines in benzidine rearrangements have been verified clearly as [5,5]- and [3,3]-sigmatropic shifts, respectively. However, to the best of our knowledge, the formations of diphenylines, *p*-semidines, and *o*-semidines seem to undergo the amphibolous pathways.¹⁸ Further unraveling the mechanisms remain highly desirable in organic chemistry. After analyzing the structures of diphenylines, *p*-semidines, and *o*-semidines and considering the existence of the C[1,3] and O[1,3]-sigmatropic shifts, we proposed that the N[1,3]-sigmatropic shift may involve in the formations of diphenylines, *p*-semidines, and *o*-semidines in the benzidine rearrangement. Herein, we present our detailed experimental and computational studies on the N[1,3]-sigmatropic shift in the formations of semidines and diphenylene in the benzidine rearrangement. We believe that our in-depth mechanistic insight of the N[1,3]-sigmatropic shift in the benzidine rearrangement is critical not only to understand the benzidine rearrangement completely, but also to enrich the theory of heteroatom [1,3]-sigmatropic shifts.

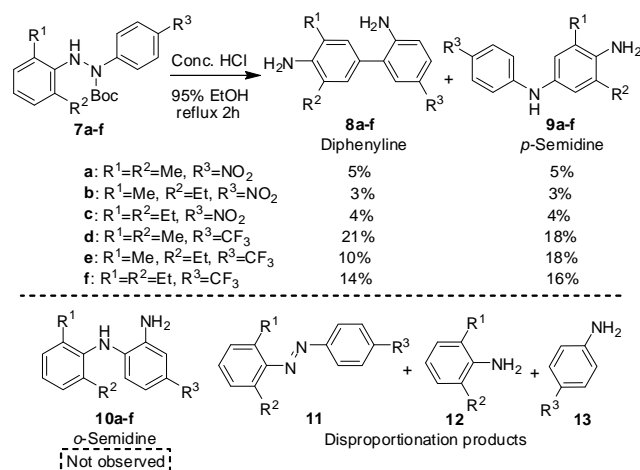
Results and discussion

Experimental Investigation on the Acid-catalyzed Semidines and Diphenylene Rearrangements

Since the benzidine rearrangements can undergo a concerted [5,5]-sigmatropic rearrangement to produce *p*-benzidines as major products, or a [3,3]-sigmatropic shift to yield *o*-benzidines, we designed *N,N'*-diaryl hydrazines with 2,4',6-substituents in order to prevent the formation of *p*-benzidine and *o*-benzidine products, simplifying the separation and determination of the rearrangement products. *N,N'*-Diaryl hydrazines **7** with different substituents were synthesized from 2,6-disubstituted *N'*-Boc-*N*-aryl hydrazines and 4-substituted aryl halides by the Cu (I)-catalyzed coupling reaction.¹⁹

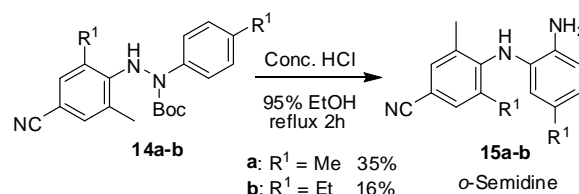
We envisioned that the 2,4',6-trisubstituted *N,N'*-diaryl hydrazines **7** would give rise to semidines and diphenylines (Scheme 2). *N,N'*-Diaryl hydrazine **7a** was first examined upon reflux in 95% ethanol for 2 h in the presence of concentrated HCl. After workup, we obtained the expected diphenylene **8a** in 5% yield and *p*-semidine **9a** in 5% yield, concomitant with the disproportionation products such as azobenzene **11a** and corresponding arylamines **12a** and **13a**. However, no *o*-semidine type product **10a** was observed. Other two nitro substituted *N,N'*-diaryl hydrazines **7b-c** gave the similar results. With trifluoromethyl substituent, *N,N'*-diaryl hydrazines **7d-f** underwent the acid-catalyzed rearrangement to provide better results, affording 10~21% yields of the diphenylines **8d-f** and 16~18% yields of *p*-semidines **9d-f** with the corresponding

disproportionation products (see ESI for details). Moreover, all reactions were subjected to the LC-MS analysis without the observation of the *o*-semidines **10**.



Scheme 2 Acid-catalyzed rearrangement of 2,4',6-trisubstituted *N,N'*-diarylhydrazines **7**.

To obtain *o*-semidine type products, we designed 2,4,4',6-tetrasubstituted *N,N'*-diaryl hydrazines **14**, which would suppress the formation of diphenylene and *p*-semidine products. Similarly, *N,N'*-diaryl hydrazines **14** were synthesized from 2,4,6-trisubstituted *N'*-Boc-*N*-aryl hydrazines and 4-substituted aryl halides via the Cu (I)-catalyzed coupling reaction. To our delight, the substrates **14a** and **14b** underwent the acid-catalyzed rearrangement to obtain the designed *o*-semidine type products **15a** and **15b** in 35% and 16% yields, respectively (Scheme 3), concomitant with the disproportionation products **13**, **16** and **17** (see ESI for details).



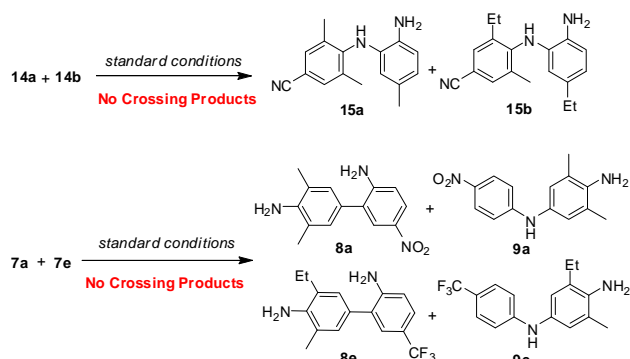
Scheme 3 Acid-catalyzed rearrangement of 2,4,4',6-tetrasubstituted *N,N'*-diarylhydrazines **14**.

Therefore, 2,4',6-trisubstituted *N,N'*-diaryl hydrazines underwent the acid-catalyzed rearrangement to produce diphenylene type products (up to 21% yield) and *p*-semidine type products (up to 18% yield), while 2,4,4',6-tetrasubstituted *N,N'*-diaryl hydrazines gave rise to *o*-semidine type products (up to 35% yield). In all the acid-catalyzed rearrangements, competitive disproportionation reactions were inevitable.

Control Experiments

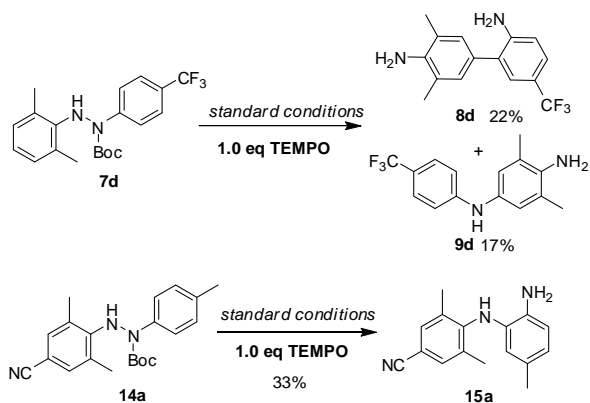
It is unclear that the formations of semidines and diphenylines are intramolecular or intermolecular processes, although it is well-known that the benzidine rearrangement is an intramolecular reaction for the formation of *o*- and *p*-benzidines.²⁰ We performed the intercrossing experiments to clarify the mechanism

(Scheme 4). A mixture of equimolar amounts of *N,N'*-diaryl hydrazines **14a** and **14b** was treated under the standard conditions. Only two *o*-semidines **15a** and **15b** were detected without the intercrossing *o*-semidines, as determined by LC-MS analysis (see ESI for details). Likewise, the intercrossing experiment with equimolar amounts of the *N,N'*-diaryl hydrazines **7a** and **7e** was conducted to offer two diphenylines **8a** and **8e**, as well as two *p*-semidines **9a** and **9e** without any intercrossing products (see ESI for details). No intercrossing products indicate that all rearrangements are intramolecular processes.



Scheme 4 Intercrossing experiments for the formation of *o*-semidines, *p*-semidines, and diphenylines

To rule out the solvent-caged biradical mechanism of the rearrangements, the radical trapping experiments were performed as well (Scheme 5). Treatment of hydrazine **7d** under the standard conditions with TEMPO gave rise to diphenylene **8d** in 22% yield and *p*-semidine **9d** in 17% yield. Hydrazine **14a** afforded *o*-semidine **15a** in 33% yield with TEMPO under the standard conditions. The radical trapper has no significant effect on the conversion of the rearrangements, excluding the radical-free process reported by Shine.¹⁵ The results indicate that even the biradicals were generated, they formed disproportionation products rather than semidines and diphenylines.



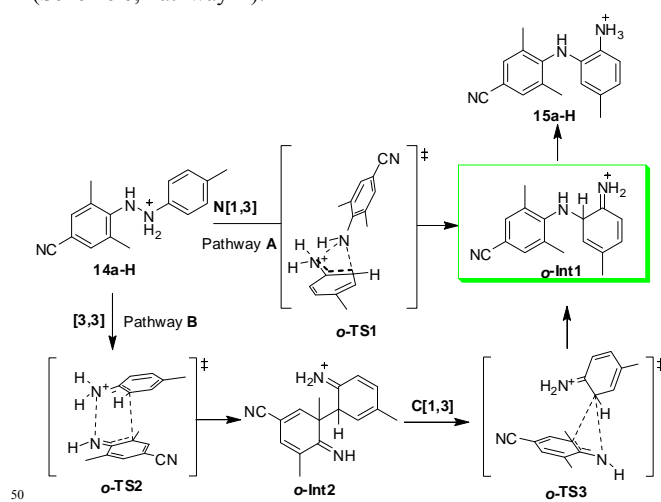
Scheme 5 Radical trapping experiments in the formation of *o*-semidine, *p*-semidine, and diphenylene type products.

30 Computational Studies

DFT calculations²¹ using the B3LYP/6-311++G(d,p) level were employed to locate all the stationary points involved.²² Frequency calculations at the same level were performed to

confirm each stationary point to be either an intermediate or a transition state structure. The free energies in solution were computed by a self-consistent reaction field (SCRF) using the conductor polarizable continuum model (CPCM) method in ethanol at the same level.²³

***o*-Semidine Rearrangement.** Our intercrossing and radical trapping experiments have excluded the ionic and radical mechanisms. Thus, the formation of *o*-semidine products should be an intramolecular process in the acid-catalyzed benzidine rearrangement. We proposed two possible intramolecular mechanisms for the *o*-semidine rearrangement: 1) a concerted N[1,3]-sigmatropic shift with a configuration inversion of the nitrogen atom, which is orbital symmetry allowed (Scheme 6, Pathway A); 2) a tandem [3,3]- and C[1,3]-sigmatropic shifts process with a configuration inversion of the carbon atom (Scheme 6, Pathway B).



Scheme 6 Proposed mechanism of the *o*-semidine rearrangement.

To understand the above possible mechanisms, mono-protonated hydrazine **14a-H** as a representative model system was examined with the DFT calculation (Figure 2). Diprotonated hydrazine **14a-2H** was also taken into account, whereas the scission of the N-N bond took place spontaneously possibly due to the unstable vicinal dicationic structure. Another mono-protonated hydrazine **14a-H'** is unstable over **14a-H** by 1.6 kcal/mol in the terms of Gibbs free energy due to protonation on the weaker basic nitrogen atom. **14a-H** undergoes the concerted N[1,3]-sigmatropic shift through a transition state **o-TS1** with an activation free energy of 11.0 kcal/mol to afford a stable intermediate **o-Int1** (Pathway A). In the **o-TS1**, the computed distances of the N-N bond breaking and the N-C bond making are 2.75 and 2.95 Å, respectively (Figure 3). The alternative Pathway B involves the [3,3]-sigmatropic shift via a transition state **o-TS2** with an activation free energy of 20.4 kcal/mol, leading to an intermediate **o-Int2**. The distances of the N-N bond cleavage and the C-C bond formation in the **o-TS2** are 2.83 and 2.13 Å, respectively (Figure 3). The following C[1,3]-sigmatropic shift via a transition state **o-TS3** is almost barrierless to form the **o-Int1**. In the **o-TS3**, the computed C-C and C-N bonds in the four-membered ring transition state are almost dissociated due to the rigid ring. Finally, the assistance of water molecule facilitates the tautomerization from the **o-Int1** to **15a-H**.

In addition, the potential profiles from **14a-H** were attempted to be calculated for sake of comparison. However, unfortunately, its *o*-**TS1** cannot be located. On the other hand, the two stereoisomers of the *o*-**TS1** were also considered in calculation (Fig. 2). When optimization, the potential energy of the *o*-**TS1** with *exo*-H decreased continuously till the *o*-**TS1** with *endo*-H because the *endo*-H *o*-**TS1** shows less steric hindrance than *exo*-H one. Additionally, a weak H- π interaction exists in the *endo*-H *o*-**TS1** due to the distance of H and the benzene ring approximate 2.6 Å (see ESI for details) and without the repelling interaction between the lone pair of electrons on the nitrogen and the π electron cloud of benzene ring (or called cyclohexadiene part). Both steric and electronic effects indicate that the transition state *endo*-H *o*-**TS1** is more stable than the *exo*-H *o*-**TS1**. A similar phenomenon was observed in the *o*-**TS3**. The results indicate that the steric hindrance plays an important role in the stabilization of the *endo*-H transition states in both N and C[1,3] sigmatropic shifts.

The distortion/interaction analysis,²⁴ which is a powerful tool to understand the factors that stabilize the transition states, was employed to allow for deep understanding of the main reasons why *o*-**TS1** is lower in energy than *o*-**TS2** (Fig. 3). The activation energy (ΔE^\ddagger) can be mainly separated into the distortion energy of anilines ($\Delta E_{\text{dist}}^\ddagger$) and the interaction energy between two distorted fragments ($\Delta E_{\text{int}}^\ddagger$). In *o*-**TS1**, the interaction energy between the two fragments is very small, but both fragments are hardly distorted from initial equilibrium geometries. In contrast, there is much more distortion of the fragments in *o*-**TS2**, and this is only partially compensated for by more effective interaction. Thus, the pathway through *o*-**TS1** is favorable for the *o*-semidine rearrangement, dominantly attributed to low distortion in the transition state.

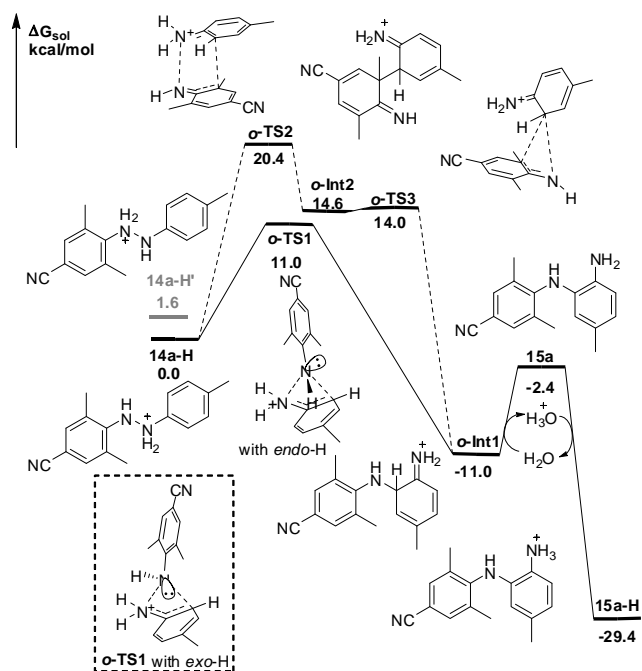


Fig. 2. Free energy profiles for the *o*-semidine rearrangement.

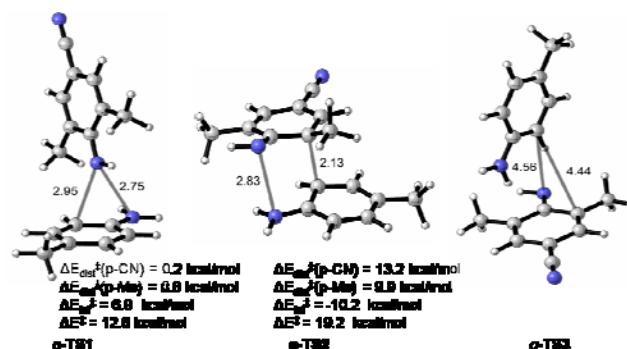
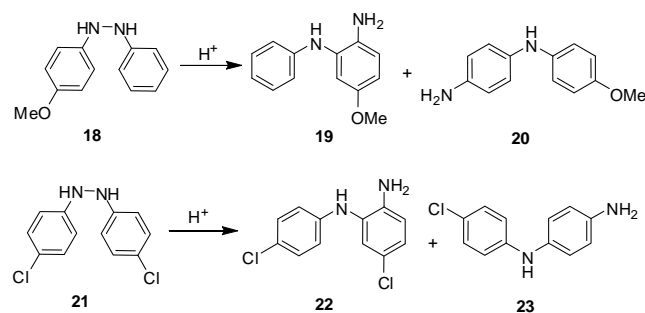


Fig. 3. Structures and distortion/interaction analysis of transition states for the *o*-semidine rearrangement. Distances of concern are reported in angstroms.

In terms of the *o*-semidine rearrangement, Shine and co-workers have reported KIE for the rearrangements of *N*-4-methoxyphenyl-*N*'-phenylhydrazine (**18**)^{15a} and *N,N'*-di(4-chlorophenyl)hydrazine (**21**) (Scheme 7).^{15b-d} The formation of *o*-semidine **19** from [¹⁵N,¹⁵N']-**18** resulted in an averaged KIE of 1.074, while the generation of *o*-semidine **22** from [¹⁴N,¹⁵N']-**21** and [2,2',6,6'-¹³C₄]-**21** furnished KIEs of 1.0155 and 0.9963, respectively. The ¹⁵N KIE is more obvious than ¹³C KIE, even an inverse ¹³C kinetic isotope effect was observed close to unity. The KIE results indicate that the transition state in the rate-determining step should be an early (reactant-like) transition state rather than a late transition state, consistent with the calculated results because the *o*-**TS1** in the N[1,3] sigmatropic shift is an early transition state, while the *o*-**TS2** in the [3,3] sigmatropic shift is a late transition state. Thus, Shine's KIE results support the N[1,3]-sigmatropic shift mechanism for the formation of *o*-semidine.



Scheme 7. Acid-catalyzed rearrangement of *N,N'*-diarylhazines **18** and **21**.

Diphenylene and *p*-Semidine Rearrangements. For the diphenylene rearrangement, we put forward two possible intramolecular but stepwise pathways: tandem N[1,3]/[3,3]-sigmatropic shifts (Pathway **C1**) and cascade [3,3]/C[1,3]-sigmatropic shifts (Pathway **D1**). For the formation of *p*-semidines, we also propose two possible intramolecular but stepwise pathways: tandem N[1,3]/N[1,3]-sigmatropic shifts (Pathway **C2**) and cascade [3,3]/[3,3]-sigmatropic shifts (Pathway **D2**) (Scheme 8).

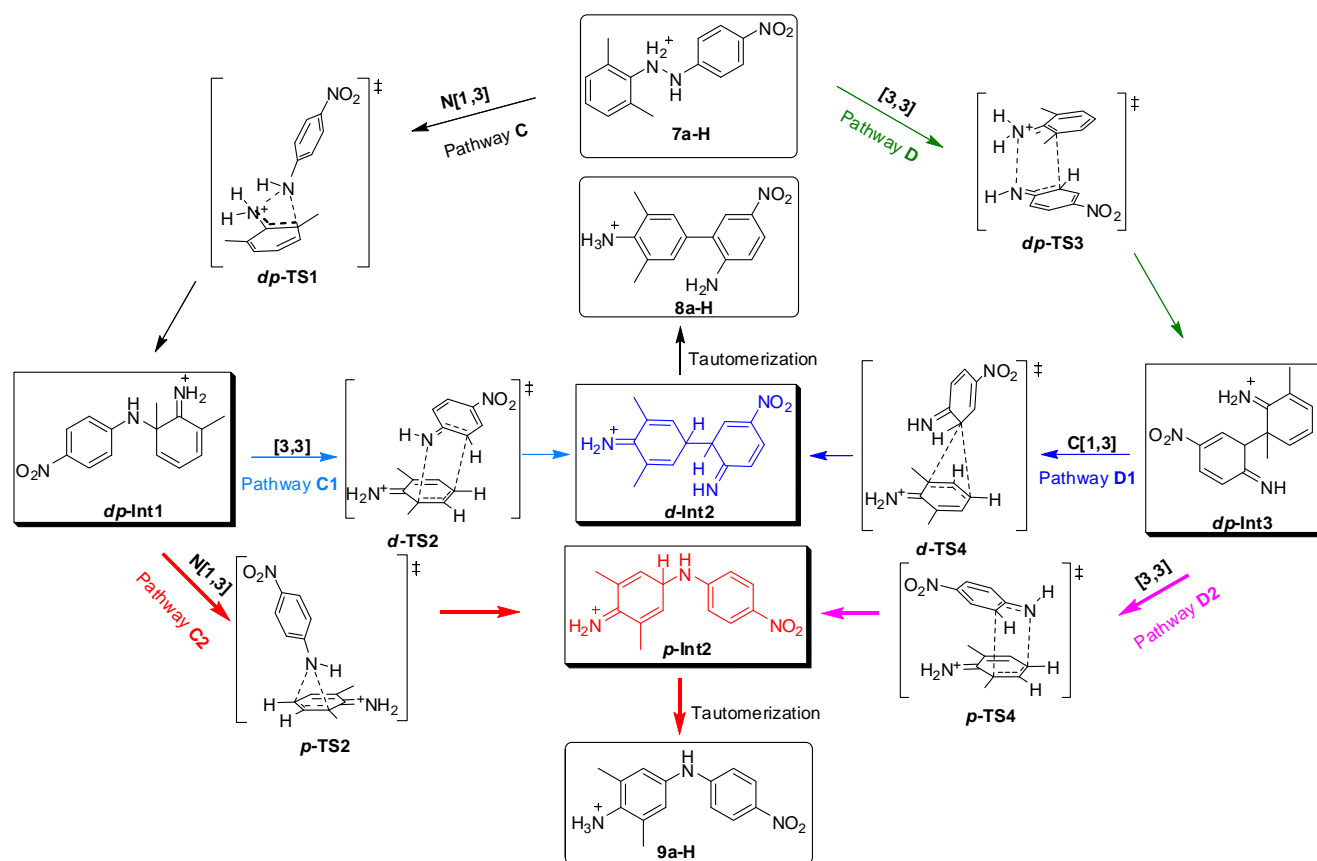
A representative model system with mono-protonated hydrazine **7a-H** was examined with DFT calculation to understand the proposed pathways (Figure 4). **7a-H** could undergo the N[1,3]-sigmatropic shift via a transition state *dp*-**TS1**

with an activation free energy of 17.0 kcal/mol. This step of the reaction is exergonic by 15.8 kcal/mol, giving a stable intermediate **dp-Int1** (pathway C). Once the intermediate **dp-Int1** is formed, two pathways can be followed: (i) the [3,3]-sigmatropic shift of **dp-Int1** via a transition state **d-TS2** requires an activation energy of 31.5 kcal/mol (but only 15.7 kcal/mol in terms of the Gibbs free energy) to yield an unstable intermediate **d-Int2**, followed by tautomerization to deliver mono-protonated diphenylene **8a-H** (pathway C1); (ii) **dp-Int1** undergoes another N[1,3]-sigmatropic shift via a transition state **p-TS2**, requiring an activation energy of 36.3 kcal/mol (20.5 kcal/mol in terms of the Gibbs free energy) to give rise to a stable intermediate **p-Int2** (pathway C2). Alternatively, **7a-H** could also undergo a [3,3]-sigmatropic shift via a transition state **dp-TS3** with an activation energy of 24.2 kcal/mol to yield an unstable intermediate **dp-Int3** (Pathway D), which can further undergo two different rearrangements: (i) the consequent C[1,3]-sigmatropic shift of **dp-Int3** through **d-TS4** requires 32.9 kcal/mol in terms of the Gibbs free energy (the activation energy of 16.2 kcal/mol), leading to **8a-H** (Pathway D1); (ii) the [3,3]-sigmatropic shift of **dp-Int3** results in the formation of **9a-H** with an activation energy of 5.0 kcal/mol (21.7 kcal/mol in terms of the Gibbs free energy) (Pathway D2).

Therefore, pathway C is more favored over pathway D by 7.2 kcal/mol in the first step of the tandem processes and predominant in each of the second steps in terms of the Gibbs

free energy. Although the two second steps in pathway D could occur with relative lower activation energies (16.2 kcal/mol and 5.0 kcal/mol, respectively) than those in pathway C, it is very difficult for the first step reaction in pathway D due to its higher activation energy (24.2 kcal/mol) and endergonic process. However, the intermediate **dp-Int1** is more stable than **dp-Int3** by 32.5 kcal/mol. In the consequent step from **dp-Int1**, two different pathways can correspond to mono-protonated diphenylene **8a-H** (pathway C1) and mono-protonated *p*-semidine **9a-H** (pathway C2). Eventually, our calculated results draw the conclusion that the first N[1,3] shift is the rate-limiting step for the formation of diphenylene **8a**, while the second N[1,3] shift is both the rate-limiting and the rate-determining step for the generation of *p*-semidine **9a**. The computed distances of all transition states are in reasonable range except for those of **d-TS4** reach the extent of scission (Figure 5).

Shine and co-workers had reported the KIEs for the rearrangement of *N,N'*-diphenylhydrazine (**1**) into diphenylene (**3**).^{13e,14c} The KIEs for [¹⁵N,¹⁵N']-**1** and [2,2',6,6'-¹³C₄]-**1** are 1.0367 and 0.9953, respectively. For [4,4'-¹³C₂]-**1**, no carbon KIE was observed. These findings imply that the cleavage of the N-N bond and the formation of the N-C2 bond are in the rate-limiting step. Similarly, more obvious ¹⁵N KIE (variation magnitude) was observed than ¹³C KIE, an inverse ¹³C KIE. The KIE results reveal that the transition state in the rate-limiting step should be an early (reactant-like) transition state rather than a late transition



Scheme 8. Proposed mechanism for diphenylene and *p*-semidine rearrangements.

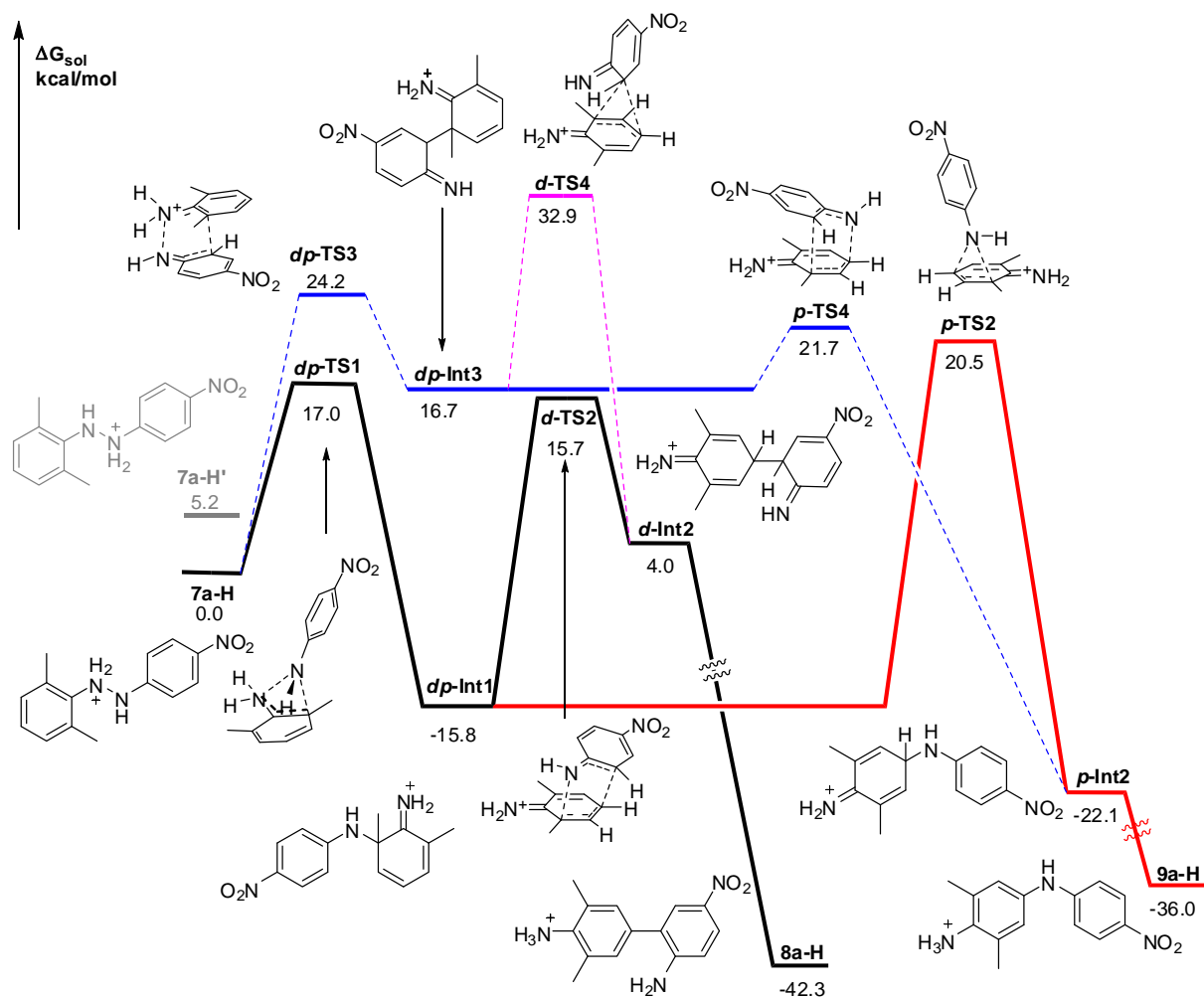


Fig. 4. Potential energy profiles of the diphenylene and *p*-semidine rearrangements.

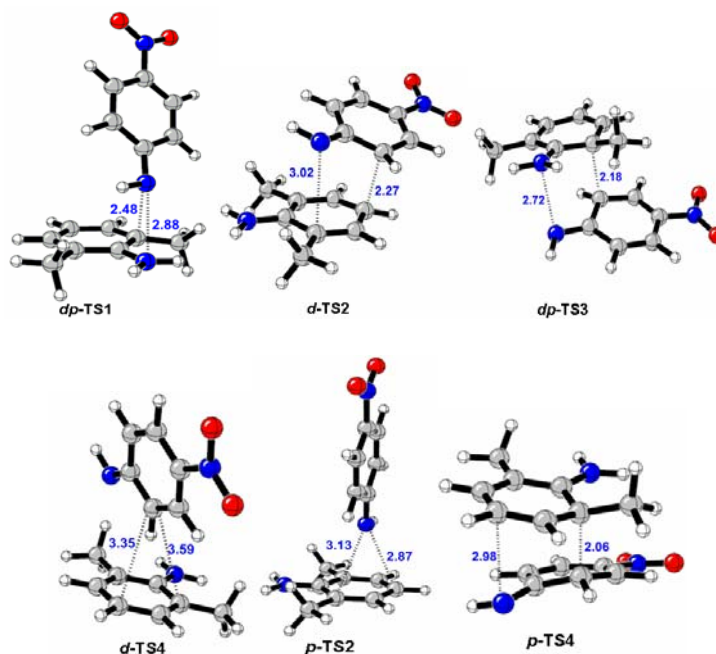


Fig. 5. Structures of transition states for the *p*-semidine and diphenylene rearrangements. Distances of concern are reported in angstroms.

Table 1. The calculated energies of transition states and intermediates in the formation of diphenylines and semidines from different diarylhydrazines in the pathways A and C (ΔG and ΔG^\ddagger in kcal/mol).

Hydrazine	ΔG^\ddagger (<i>o</i> -TS1)	ΔG (<i>o</i> -Int1)	ΔG^\ddagger (<i>dp</i> -TS1)	ΔG (<i>dp</i> -Int1)	ΔG^\ddagger (<i>d</i> -TS2)	ΔG (<i>d</i> -Int2)	ΔG^\ddagger (<i>p</i> -TS2)	ΔG (<i>p</i> -Int2)
14a	11.0	-11.0	-	-	-	-	-	-
7a	-	-	17.0	-15.0	15.7	4.0	20.5	-22.1
1	14.7	-13.0	14.7	-13.0	15.0	4.7	NL	NC
18	14.2	-8.9	14.8	1.7	NL	NC	16.4	-12.4
21	12.8	-10.8	12.8	-10.8	NL	NC	13.3	-19.1

NL = Not located. NC = Not calculated.

state, consistent with our calculated tandem N[1,3]/[3,3] sigmatropic shift mechanism with the first N[1,3] sigmatropic shift as the rate-limiting step because the *dp*-TS1 in the first N[1,3] sigmatropic shift is an early transition state with a higher potential energy of 17.0 kcal/mol, while the *d*-TS2 in the second [3,3] sigmatropic shift is a late transition state. On the other hand, the transition state *dp*-TS3 is a late transition state and locates at a higher potential energy of 24.2 cal/mol as well. Although *d*-TS4 is also an early transition state, but with the highest potential energy of 32.9 cal/mol. After this analysis, we can conclude that our proposed tandem N[1,3]/[3,3]-sigmatropic shifts and the first N[1,3] sigmatropic shift as the rate-limiting step for the formation mechanism of the diphenylines are consistent with Shine's KIE observation.

The averaged KIEs for the formation of *p*-semidine **20** from [¹⁵N, ¹⁵N²]-**18** and [4²-¹⁴C]-**18** were measured as 1.0296 and 1.039, respectively.^{15a,d} On the basis of the KIE results, a concerted [1,5]-sigmatropic shift through a six-membered ring transition state from the protonated **18** was proposed by Shine. However, the proposed transition state for the concerted [1,5]-sigmatropic shift seems to have large distorted energy with the rigid benzene ring. It is not a reasonable process. However, the KIEs support our tandem N[1,3]/N[1,3] sigmatropic shift process and the second one as the rate-limiting step.

In addition, the formation of *p*-semidine **23** from [¹⁵N, ¹⁵N²]-**21**, [¹⁴N, ¹⁵N²]-**21**, [4,4²-¹³C₂]-**21**, [4-¹⁴C]-**21**, and [2,2²,6,6²-¹³C₄]-**21** furnished KIEs of 1.0282, 1.0162, 0.9934, 1.0029, and 0.9973, respectively.^{15b-d} The results indicate that the rate-limiting step involves the nitrogen atom, ortho and para carbon atoms, also matched with our proposed tandem N[1,3]/N[1,3]-sigmatropic shifts mechanism with the second N[1,3]-sigmatropic shift as the rate-limiting step for the formation of *p*-semidine. From viewpoint of energy, it is reasonable to consider the formation mechanism of *p*-semidines as tandem N[1,3]/N[1,3]-sigmatropic shifts mechanism with the second N[1,3]-sigmatropic shift as the rate-limiting step. However, the carbon KIEs for both ortho and para carbon atoms are very small, unlike the transition states *o*-TS1 and *dp*-TS1, no obvious relationship between their variation magnitudes and the transition state structure of *p*-TS2 is observed due to the experimental determination precision. The small carbon KIEs are possibly attributed to the rigid benzene ring involved in the transition state *p*-TS2. Small carbon KIEs were observed in several cyclic transition states previously.²⁵⁻²⁷

In the rearrangements of diphenylines, *o*- and *p*-semidines, the inverse carbon KIE is generally observed. Unlike deuterium KIE, the heavy atom primary inverse KIEs have seldom observed previously.²⁸ They were assumed to generate due to nonlinear in the transition states, causing bending modes in addition to

stretching modes in vibrations. In our investigated rearrangements, all the transition states in the rate-limiting steps are four-membered ring ones. Thus, the inverse carbon KIE can be attributable to the nonlinear transition states in the rate-limiting steps.

Influence of Substituents on Transition States and KIEs.

The substituents can change the transition states (early or late transition states), resulting in KIE changes, even normal to inverse or inverse to normal.²⁸ Our investigated *N,N'*-diarylhydrazines are different from those in the KIE experiments. To verify the impact of the substituents on the phenyl group(s) on the transition states in the semidine and diphenylene rearrangements, we further calculated the potential energy profiles for the formation of semidines and diphenylines from *N,N'*-diarylhydrazines **1**, **18**, and **21** (Table 1). The results indicated that all the transition states *o*-TS1 for *N,N'*-diarylhydrazines **14a**, **1**, **18**, and **21** are early transition states (Table 1, columns 1 and 2), indicating that these diarylhydrazines should show similar ¹⁵N and ¹³C KIEs in their *o*-semidine rearrangements. That is, the reported KIEs of **18** and **21** can represent those in our studied system of *N,N'*-diarylhydrazine **14a**.

For *p*-semidine rearrangements, except for *N,N'*-diphenylhydrazine **1**, of which *p*-TS2 cannot be located in its calculation (consistent with trace *p*-semidine **5** generated in the experiment), the transition states *p*-TS2 for both *N,N'*-diarylhydrazines **18** and **21** show higher potential energy than the corresponding *dp*-TS1 and are early transition states, indicating that the second N[1,3] sigmatropic shift is the rate-limiting step in the formation of the corresponding *p*-semidines **20** and **23** as that in the formation of *p*-semidine **9a**. The hydrazine **21** shows similar potential energy profile to that of the hydrazine **7a** in the *p*-semidine rearrangement. Thus, the KIEs of **21** should represent those of **7a**. However, the hydrazine **21** possesses lower energy barriers than **7a** in both N[1,3] sigmatropic shifts. That is the reason why **7a** yields **9a** in a low yield of 5%, while **21** generated **23** in a relatively high yield of 12%.

Considering the diphenylene rearrangements, the transition states *d*-TS2 are not located in their calculation for hydrazines **18** and **21**, in agreement with no observation of the corresponding diphenylines experimentally. Thus, only *N,N'*-diphenylhydrazine **1** was compared with hydrazine **7a**. However, the unexpected results were obtained. For hydrazine **7a**, its transition state *d*-TS2 is slightly higher (0.3 kcal/mol) than its *dp*-TS1 in terms of the Gibbs free energy, but a less obvious difference on the viewpoint of calculation. Importantly, the *dp*-TS1 of hydrazine **1** is an early transition state as that in hydrazine **7a**. It is matched with the variation magnitudes of its ¹⁵N and ¹³C KIEs. The KIEs of hydrazine **1** could reflect the feature of the diphenylene

rearrangements. Although it is difficult to provide an undoubted mechanism for the formation of diphenylnes in the benzidine rearrangement on the basis of the current information, our proposed mechanism is more reasonable one till now and our current investigation provides a further new insight and comprehensive understanding on the *o*- and *p*-semidines and diphenylene rearrangements.

Conclusion

In summary, to search for the existence of the N[1,3]-sigmatropic shift and to further elucidate the formation mechanisms of *o/p*-semidines and diphenylnes, we have investigated the mechanisms for the acid-catalyzed semidines and diphenylene rearrangements with designed *N,N'*-diarylhydrazines. After a systematic investigation on experiments and theoretical calculations, it is reasonable to consider the acid-catalyzed *o*-semidine rearrangement as a N[1,3]-sigmatropic shift, *p*-semidine rearrangement as tandem N[1,3]/N[1,3]-sigmatropic shifts, and diphenylene rearrangement as cascade N[1,3]/[3,3]-sigmatropic shifts. The N[1,3]-sigmatropic shift is orbital suprafacial symmetry allowed with an inversion of the migrating nitrogen atom. The proposed intramolecular processes are supported by intercrossing experiments, radical trapping experiments, and KIE observation measured by Shine. The current results not only provide a comprehensive understanding on the formation of *o/p*-semidines and diphenylnes in the benzidine rearrangement, but also disclose a novel N[1,3]-sigmatropic shift that has potential mechanistic possibility in other reactions.

Experimental section

General information

Melting points were obtained on a melting point apparatus and are uncorrected. ¹H NMR and ¹³C NMR spectra were recorded on a 300 MHz or 400 MHz spectrometer with TMS as an internal standard in the CDCl₃ solution. IR spectra were taken on a FT-IR spectrometer in KBr. HRMS data were obtained with an LC/MSD TOF mass spectrometer. Purification of reaction products was carried out by column chromatography using silica gel (200–300 mesh). TLC separations were performed on silica gel G plates with petroleum ether/ethyl acetate, and the plates were visualized with UV light.

General procedure for the synthesis of *N*-Boc-*N,N'*-diarylhydrazines **7** and **14**

To a round bottom flask were charged with an *N'*-Boc-*N*-aryl hydrazines (**24**, 48 mmol), 4-substituent iodobenzene (40 mmol), CuI (0.78 g, 4 mmol), 1,10-phenanthroline (1.44 g, 8 mmol), Cs₂CO₃ (15.64 g, 48 mmol) and 40 mL of dry DMF at room temperature. The reaction mixture was degassed, charged with N₂ gas and heated to 80 °C. After 4–5 hrs, the resulting mixture was cooled to room temperature, diluted with ethyl acetate (100 mL), filtered. The filtrate was then washed twice with brine (2×100 mL). The organic layer was dried over anhydrous magnesium sulfate, filtered, concentrated under reduced pressure. The residue was purified by flash chromatography with a mixture of petroleum ether and ethyl acetate as an eluent to afford the desired product, which was recrystallized from a mixture of

petroleum ether and ethyl acetate to give crystals **7** or **14**.

tert-Butyl 2-(2,6-dimethylphenyl)-1-(4-nitrophenyl)hydrazinecarboxylate (7a). Orange crystals, 2.57 g, yield 18%, m.p. 153–154 °C, ¹H NMR (300 MHz, CDCl₃) δ: 1.27 (s, 9 H), 2.17 (s, 6 H), 6.27 (s, 1H), 6.82 (t, *J* = 7.4 Hz, 1 H), 6.97 (d, *J* = 7.4 Hz, 2 H), 8.07–8.12 (m, 2 H), 8.19–8.25 (m, 2 H). ¹³C NMR (75 MHz, CDCl₃) δ: 153.3, 149.3, 143.3, 142.8, 129.7, 124.8, 124.1, 121.9, 119.7, 83.7, 27.6, 19.0. IR (KBr) ν (cm⁻¹): 3359, 2978, 2932, 1721, 1590, 1514, 1476, 1308. HRMS (ESI) calcd. for C₁₉H₂₃N₃O₄ [M+H]⁺ *m/z*: 358.1761, found 358.1769.

tert-Butyl 2-(2-ethyl-6-methylphenyl)-1-(4-nitrophenyl)hydrazinecarboxylate (7b). Orange crystals, 2.38 g, yield 16%, m.p. 118–119 °C, ¹H NMR (300 MHz, CDCl₃) δ: 1.19 (t, *J* = 7.5 Hz, 3 H), 1.26 (s, 9 H), 2.15 (s, 3 H), 2.56 (q, *J* = 7.5 Hz, 2 H), 6.34 (s, 1H), 6.85–7.03 (m, 3 H), 8.06–8.12 (m, 2 H), 8.20–8.25 (m, 2 H). ¹³C NMR (50 MHz, CDCl₃) δ: 153.4, 149.4, 143.0, 142.8, 131.2, 129.8, 127.3, 125.3, 124.1, 122.1, 119.8, 83.7, 27.6, 24.7, 19.5, 14.2. IR (KBr) ν (cm⁻¹): 3359, 2974, 2932, 2875, 1716, 1590, 1515, 1469, 1342, 1113. HRMS (ESI) calcd. for C₂₀H₂₅N₃O₄ [M+H]⁺ *m/z*: 372.1918, found 372.1914.

tert-Butyl 2-(2,6-diethylphenyl)-1-(4-nitrophenyl)hydrazinecarboxylate (7c). Orange crystals, 2.00 g, yield 13%, m.p. 164–165 °C, ¹H NMR (300 MHz, CDCl₃) δ: 1.15 (t, *J* = 7.5 Hz, 6 H), 1.26 (s, 9 H), 2.52 (q, *J* = 7.5 Hz, 4 H), 6.37 (s, 1 H), 6.94–7.04 (m, 3 H), 8.07–8.12 (m, 2 H), 8.21–8.26 (m, 2 H). ¹³C NMR (50 MHz, CDCl₃) δ: 153.5, 149.4, 143.2, 142.3, 131.9, 127.3, 124.1, 122.6, 120.1, 83.8, 27.7, 24.9, 14.4. IR (KBr) ν (cm⁻¹): 3349, 2983, 1721, 1589, 1492, 1441, 1339. HRMS (ESI) calcd. for C₂₁H₂₇N₃O₄ [M+H]⁺ *m/z*: 386.2074, found 386.2089.

tert-Butyl 2-(2,6-dimethylphenyl)-1-(4-(trifluoromethyl)phenyl)hydrazinecarboxylate (7d). Colorless crystals, 5.63 g, yield 37%, m.p. 105–106 °C, ¹H NMR (300 MHz, CDCl₃) δ: 1.28 (s, 9 H), 2.19 (s, 6 H), 6.23 (s, 1 H), 6.80 (t, *J* = 7.5 Hz, 1 H), 6.95 (d, *J* = 7.5 Hz, 2 H), 7.59 (d, *J* = 8.7 Hz, 2 H), 7.95 (d, *J* = 8.7 Hz, 2 H). ¹³C NMR (50 MHz, CDCl₃) δ: 153.8, 146.7, 143.6, 129.6, 125.3 (q, *J*₁ = 3.8 Hz), 125.2 (q, *J*₂ = 32.5 Hz), 125.0, 124.3 (q, *J*₃ = 270 Hz), 121.6, 120.4, 82.8, 27.6, 18.9. IR (KBr) ν (cm⁻¹): 3340, 2982, 1697, 1618, 1525, 1474, 1323. HRMS (ESI) calcd. for C₂₀H₂₃F₃N₂O₂ [M+H]⁺ *m/z*: 381.1784, found 381.1799.

tert-Butyl 2-(2-ethyl-6-methylphenyl)-1-(4-(trifluoromethyl)phenyl)hydrazinecarboxylate (7e). Colorless crystals, 7.10 g, yield 45%, m.p. 121–121.5 °C, ¹H NMR (300 MHz, CDCl₃) δ: 1.18 (t, *J* = 7.5 Hz, 3 H), 1.28 (s, 9 H), 2.17 (s, 3 H), 2.56 (q, *J* = 7.5 Hz, 2 H), 6.30 (s, 1H), 6.84–7.02 (m, 3 H), 7.58–7.61 (m, 2 H), 7.93–7.96 (m, 2 H). ¹³C NMR (50 MHz, CDCl₃) δ: 153.9, 146.6, 143.0, 131.4, 129.7, 127.2, 125.5, 125.5 (q, *J*₂ = 32.5 Hz), 125.4 (q, *J*₃ = 3.7 Hz), 124.3 (q, *J*₁ = 270 Hz), 122.0, 120.7, 83.0, 27.7, 24.7, 19.5, 14.3. IR (KBr) ν (cm⁻¹): 3367, 2975, 2932, 2869, 1720, 1615, 1469, 1322, 1160, 1115. HRMS (ESI) calcd. for C₂₁H₂₅F₃N₂O₂ [M+H]⁺ *m/z*: 395.1941, found 395.1937.

tert-Butyl 2-(2,6-diethylphenyl)-1-(4-(trifluoromethyl)phenyl)hydrazinecarboxylate (7f). Colorless crystals, 4.41 g, yield 27%, m.p. 83–84 °C, ¹H NMR (300 MHz, CDCl₃) δ: 1.15 (t, *J* = 7.5 Hz, 6 H), 1.27 (s, 9 H), 2.54 (q, *J* = 7.5 Hz, 4 H), 6.34 (s, 1H), 6.90–7.03 (m, 3 H), 7.58–7.61 (m, 2 H), 7.92–7.95 (m, 2 H). ¹³C NMR (50 MHz, CDCl₃) δ: 154.1, 146.7,

142.5, 132.1, 127.3, 125.7 (q, $J_2 = 32.3$ Hz), 125.4 (q, $J_3 = 3.7$ Hz), 124.3 (q, $J_1 = 270$ Hz), 122.4, 120.9, 83.0, 27.8, 24.9, 14.5. IR (KBr) ν (cm^{-1}): 3365, 2971, 2935, 2876, 1720, 1615, 1456, 1322, 1160, 1123. HRMS (ESI) calcd. for $\text{C}_{22}\text{H}_{27}\text{F}_3\text{N}_2\text{O}_2$ $[\text{M}+\text{H}]^+$ m/z : 409.2097, found 409.2086.

tert-Butyl 2-(4-cyano-2,6-dimethylphenyl)-1-(p-tolyl)hydrazinecarboxylate (14a). Colorless crystals, 4.50 g, yield 32%, m.p. 157-159 °C, ^1H NMR (300 MHz, CDCl_3) δ : 1.33 (s, 9 H), 2.23 (s, 6 H), 2.32 (s, 3 H), 6.43 (s, 1 H), 7.14 (m, 2 H), 7.21 (s, 2 H), 7.47 (m, 2 H). ^{13}C NMR (75 MHz, CDCl_3) δ : 154.1, 148.0, 140.4, 134.3, 133.2, 128.9, 125.6, 121.6, 119.6, 103.7, 82.5, 27.9, 20.7, 19.0. IR (KBr) ν (cm^{-1}): 3356, 2977, 2926, 2218, 1717. HRMS (ESI) calcd. for $\text{C}_{21}\text{H}_{25}\text{N}_3\text{O}_2$ $[\text{M}+\text{H}]^+$ m/z : 352.2020, found 352.2031.

tert-Butyl 2-(4-cyano-2-ethyl-6-methylphenyl)-1-(4-ethylphenyl)hydrazinecarboxylate (14b). Colorless crystals, 5.62 g, yield 37%, m.p. 164-164.5 °C, ^1H NMR (300 MHz, CDCl_3) δ : 1.20 (t, $J = 7.5$ Hz, 3 H), 1.23 (t, $J = 7.5$ Hz, 3 H), 1.33 (s, 9 H), 2.24 (s, 3 H), 2.59 (q, $J = 7.5$ Hz, 2 H), 2.64 (q, $J = 7.5$ Hz, 2 H), 6.45 (d, $J = 4.1$ Hz, 1 H), 7.17 (m, 2 H), 7.23 (s, 1 H), 7.28 (s, 1 H), 7.49 (m, 2 H). ^{13}C NMR (75 MHz, CDCl_3) δ : 154.1, 147.6, 140.5, 140.5, 133.1, 131.5, 130.8, 127.6, 126.0, 121.6, 119.7, 103.8, 82.3, 28.0, 27.8, 24.3, 19.4, 15.3, 13.6, 8.7. IR (KBr) ν (cm^{-1}): 3343, 2964, 2929, 2219, 1718. HRMS (ESI) calcd. for $\text{C}_{23}\text{H}_{29}\text{N}_3\text{O}_2$ $[\text{M}+\text{H}]^+$ m/z : 380.2333, found 380.2346.

General procedure for the acid-catalyzed rearrangements of N,N' -diaryl hydrazines **7** and **14**

To a round bottom flask were charged with an N,N' -diaryl hydrazine (**7** or **14**, 1 mmol), 95% ethanol (10 mL), and conc. HCl (0.5 mL) under nitrogen at room temperature. The reaction mixture was refluxed for 2 hrs, then cooled to room temperature, neutralized with solid NaHCO_3 , filtered, concentrated. The residue was purified by flash column chromatography.

3',5'-Dimethyl-5-nitro-1,1'-biphenyl-2,4'-diamine (8a).

Yellowish crystals, 13 mg, yield 5%, m.p. 186-188 °C, ^1H NMR (300 MHz, CDCl_3) δ : 2.23 (s, 6 H), 3.73 (s, 2 H), 4.54 (s, 2 H), 6.67 (q, $J_1 = 2.6$ Hz, 1 H), 7.01 (s, 2 H), 8.01 (dd, $J_1 = 2.6$ Hz, $J_2 = 2.3$ Hz, 2 H). ^{13}C NMR (126 MHz, CDCl_3) δ : 150.1, 142.9, 139.2, 128.6, 127.1, 126.7, 126.2, 124.5, 122.3, 113.6, 17.7. IR (KBr) ν (cm^{-1}): 3433, 3340, 2962, 2873, 1284. HRMS (ESI) calcd. for $\text{C}_{14}\text{H}_{15}\text{N}_3\text{O}_2$ $[\text{M}+\text{H}]^+$ m/z : 258.1237, found 258.1245.

3'-Ethyl-5'-methyl-5-nitro-1,1'-biphenyl-2,4'-diamine (8b).

Brown crystals, 8 mg, yield 3%, m.p. 131-133 °C, ^1H NMR (300 MHz, CDCl_3) δ : 1.29 (t, $J_1 = 7.5$ Hz, 3 H), 2.34 (s, 3 H), 2.58 (q, $J_1 = 7.5$ Hz, 2 H), 3.77 (s, 2 H), 4.55 (s, 2 H), 6.68 (dt, $J_2 = 1.6$ Hz, $J_3 = 2.7$ Hz, 1 H), 7.02 (s, 2 H), 8.00 (d, $J_3 = 2.7$ Hz, 1 H), 8.03 (d, $J_2 = 1.6$ Hz, 2 H). ^{13}C NMR (126 MHz, CDCl_3) δ : 150.3, 142.3, 138.9, 128.4, 128.0, 127.1, 126.7, 126.5, 126.2, 124.4, 122.5, 113.5, 24.2, 17.7, 12.9. IR (KBr) ν (cm^{-1}): 3482, 3376, 2966, 2873, 1307. HRMS (ESI) calcd. for $\text{C}_{15}\text{H}_{17}\text{N}_3\text{O}_2$ $[\text{M}+\text{H}]^+$ m/z : 272.1394, found 272.1410.

N,N' -(3',5'-Diethyl-5-nitro-1,1'-biphenyl-2,4'-diyl)diacetamide (8c). The isolated mixture (48 mg) of diphenylene and *p*-nitroaniline in 5 mL of $(\text{Ac})_2\text{O}$ was stirred at room temperature for 12 hrs. The resulting mixture was diluted with water (50 mL), and extracted with ethyl acetate (2 \times 50 mL). The organic layer was washed with saturated NaHCO_3 (50 mL), brine (50 mL), dried over anhydrous Na_2SO_4 , filtered, concentrated under

reduced pressure and purified by flash chromatography with a mixture of petroleum ether and ethyl acetate as an eluent to afford **8c**. Yellowish solid, 15 mg, yield 4%, m.p. 230-232 °C, ^1H NMR (300 MHz, $\text{DMSO}-d_6$) δ : 1.17(t, $J_1 = 7.5$ Hz, 6 H), 2.03 (s, 3 H), 2.10 (s, 3 H), 2.59 (q, $J_1 = 7.5$ Hz, 4 H), 7.23 (s, 2 H), 7.99 (d, $J_3 = 8.9$ Hz, 1H), 8.12 (d, $J_2 = 2.6$ Hz, 1H), 8.22 (dd, $J_2 = 2.6$ Hz, $J_3 = 8.9$ Hz, 1H), 9.34 (s, 1 H), 9.68 (s, 1 H). ^{13}C NMR (126 MHz, $\text{DMSO}-d_6$) δ : 169.1, 168.8, 143.9, 142.0, 141.3, 135.2, 135.1, 134.5, 126.4, 126.0, 125.3, 122.8, 24.4, 23.4, 22.6, 14.8. IR (KBr) ν (cm^{-1}): 3250, 3246, 2962, 2928, 2866, 2847, 1654, 1508, 1350, 1274. HRMS (ESI) calcd. for $\text{C}_{20}\text{H}_{23}\text{N}_3\text{O}_4$ $[\text{M}+\text{H}]^+$ m/z : 370.1761, found 370.1768.

3',5'-Dimethyl-5-trifluoromethyl-1,1'-biphenyl-2,4'-diamine (8d). Colorless Crystals, 59 mg, yield 21%, m.p. 74-75 °C, ^1H NMR (300 MHz, CDCl_3) δ : 2.23 (s, 6 H), 3.70 (brs, 2 H), 4.06 (brs, 2 H), 6.73 (d, $J = 9.0$ Hz, 1 H), 7.02 (s, 2 H), 7.32 (m, 2 H). ^{13}C NMR (126 MHz, CDCl_3) δ : 146.8, 142.4, 128.6, 127.5, 127.5 (q, $J = 3.6$ Hz), 127.3, 124.9 (q, $J = 270.6$ Hz), 124.7 (q, $J = 3.6$ Hz), 122.11, 120.0 (q, $J = 32.4$ Hz), 114.4, 17.6. IR (KBr) ν (cm^{-1}): 3481, 3386, 2933, 2857, 1108. HRMS (ESI) calcd. for $\text{C}_{15}\text{H}_{15}\text{F}_3\text{N}_2$ $[\text{M}+\text{H}]^+$ m/z : 281.1260, found 281.1276.

3'-Ethyl-5'-methyl-5-trifluoromethyl-1,1'-biphenyl-2,4'-diamine (8e). Yellowish oil, 29 mg, yield 10%, ^1H NMR (300 MHz, CDCl_3) δ : 1.28 (t, $J_1 = 7.5$ Hz, 3 H), 2.23 (s, 3 H), 2.58 (q, $J_1 = 7.5$ Hz, 2 H), 3.72 (brs, 2 H), 4.08 (s, 2 H), 6.75 (d, $J_2 = 8.4$ Hz, 1 H), 7.03 (s, 2 H), 7.33 (d, $J_2 = 8.4$ Hz, 1H), 7.34 (s, 1H). ^{13}C NMR (126 MHz, CDCl_3) δ : 146.8, 141.8, 128.4, 127.8, 127.6, 127.4 (q, $J = 3.6$ Hz), 127.4, 126.5, 124.9 (d, $J = 270.7$ Hz), 124.7 (q, $J = 3.7$ Hz), 122.3, 119.8 (q, $J = 32.3$ Hz), 114.4, 24.2, 17.6, 12.9. IR (KBr) ν (cm^{-1}): 3481, 3386, 2966, 2873, 1108. HRMS (ESI) calcd. for $\text{C}_{16}\text{H}_{17}\text{F}_3\text{N}_2$ $[\text{M}+\text{H}]^+$ m/z : 295.1417, found 295.1414.

3',5'-Diethyl-5-trifluoromethyl-1,1'-biphenyl-2,4'-diamine (8f).

Yellowish oil, 43 mg, yield 14%, ^1H NMR (300 MHz, CDCl_3) δ : 1.29 (t, $J_1 = 7.5$ Hz, 6 H), 2.58 (q, $J_1 = 7.5$ Hz, 4 H), 3.77 (brs, 2 H), 4.09 (brs, 2 H), 6.75 (d, $J_2 = 8.1$ Hz, 1 H), 7.04 (s, 2 H), 7.33 (d, $J_2 = 8.1$ Hz, 1 H), 7.35 (s, 1 H). ^{13}C NMR (126 MHz, CDCl_3) δ : 146.8, 141.3, 128.1, 127.8, 127.6, 127.5 (q, $J = 3.7$ Hz), 126.4, 124.9 (q, $J = 270.7$ Hz), 124.8 (q, $J = 3.7$ Hz), 120.0 (q, $J = 32.4$ Hz), 114.5, 24.3, 13.0. IR (KBr) ν (cm^{-1}): 3483, 3389, 2966, 2874, 1108. HRMS (ESI) calcd. for $\text{C}_{17}\text{H}_{19}\text{F}_3\text{N}_2$ $[\text{M}+\text{H}]^+$ m/z : 309.1573, found 309.1577.

3,5-Dimethyl- N' -(4-nitrophenyl)benzene-1,4-diamine (9a).

Orange crystals, 13 mg, yield 5%, m.p. 193-195 °C, ^1H NMR (300 MHz, CDCl_3) δ : 2.20 (s, 6 H), 3.63 (s, 2 H), 6.04 (s, 1 H), 6.71 (d, $J = 9.2$ Hz, 2 H), 6.83 (s, 2 H), 8.07 (d, $J = 9.2$ Hz, 2 H). ^{13}C NMR (126 MHz, CDCl_3) δ : 152.4, 141.0, 138.6, 129.0, 126.4, 124.8, 122.8, 112.3, 17.7. IR (KBr) ν (cm^{-1}): 3363, 2962, 1301. HRMS (ESI) calcd. for $\text{C}_{14}\text{H}_{15}\text{N}_3\text{O}_2$ $[\text{M}+\text{H}]^+$ m/z : 258.1237, found 258.1249.

N -(2-Ethyl-6-methyl-4-((4-nitrophenyl)amino)phenyl)-

acetamide (9b). The isolated mixture (36 mg) of *p*-semidine and *p*-nitroaniline in 5 mL of $(\text{Ac})_2\text{O}$ was stirred at room temperature for 12 hrs. The resulting mixture was diluted with water (50 mL), and extracted with ethyl acetate (2 \times 50 mL). The organic layer was washed with saturated NaHCO_3 (50 mL), brine (50 mL), dried over anhydrous Na_2SO_4 , filtered, concentrated under reduced pressure and purified by flash chromatography with a

mixture of petroleum ether and ethyl acetate as an eluent to afford **9b**. Yellow solid, 9 mg, yield 3%, m.p. 256-259 °C, ¹H NMR (300 MHz, DMSO-*d*₆) δ: 1.10 (t, *J* = 7.5 Hz, 3 H), 2.04 (s, 3 H), 2.12 (s, 3 H), 2.52 (q, *J* = 7.5 Hz, 2 H), 6.93 (s, 1 H), 6.96 (s, 1 H), 7.04 (m, 2 H), 8.08 (m, 2 H), 9.14 (s, 1 H), 9.22 (s, 1 H). ¹³C NMR (126 MHz, DMSO-*d*₆) δ: 168.5, 151.0, 142.3, 138.2, 137.7, 136.9, 130.5, 126.2, 120.0, 118.5, 113.2, 24.4, 22.5, 18.2, 14.4. IR (KBr) ν (cm⁻¹): 3445, 2961, 2920, 1654, 1581, 1312. HRMS (ESI) calcd. for C₁₇H₁₉N₃O₃ [M+H]⁺ *m/z*: 314.1499, found 314.1496.

3,5-Diethyl-*N*'-(4-(nitrophenyl)benzene-1,4-diamine (9c). Red oil, 12 mg, yield 4%, ¹H NMR (300 MHz, CDCl₃) δ: 1.26 (t, *J*₁ = 7.5 Hz, 6 H), 2.54 (q, *J*₁ = 7.5 Hz, 4 H), 3.69 (s, 2 H), 6.19 (s, 1 H), 6.72 (m, 2 H), 6.85 (s, 2 H), 8.06 (m, 2H). ¹³C NMR (126 MHz, CDCl₃) δ: 152.5, 139.7, 138.4, 129.5, 128.8, 126.3, 122.3, 112.2, 24.2, 12.8. IR (KBr) ν (cm⁻¹): 3353, 2956, 2866, 1306. HRMS (ESI) calcd. for C₁₆H₁₉N₃O₂ [M+H]⁺ *m/z*: 286.1550, found 286.1564.

3,5-Dimethyl-*N*'-(4-(trifluoromethyl)phenyl)benzene-1,4-diamine (9d). Colorless crystals, 50 mg, yield 18%, m.p. 115-117 °C, ¹H NMR (500 MHz, CDCl₃) δ: 2.18 (s, 6 H), 3.54 (brs, 2 H), 5.63 (brs, 1 H), 6.79 (d, *J* = 8.4 Hz, 2 H), 6.80 (s, 2 H), 7.38 (d, *J* = 8.4 Hz, 2 H). ¹³C NMR (126 MHz, CDCl₃) δ: 149.4, 139.9, 130.9, 126.5 (q, *J* = 3.5 Hz), 124.9 (q, *J* = 270.4 Hz), 124.0, 122.8, 119.6 (q, *J* = 32.3 Hz), 113.3, 17.7. IR (KBr) ν (cm⁻¹): 3382, 2929, 2853, 1109. HRMS (ESI) calcd. for C₁₅H₁₅F₃N₂ [M+H]⁺ *m/z*: 281.1260, found 281.1274.

3-Ethyl-5-methyl-*N*'-(4-(trifluoromethyl)phenyl)benzene-1,4-diamine (9e). Yellowish oil, 53 mg, yield 18%, ¹H NMR (300 MHz, CDCl₃) δ: 1.25 (t, *J*₁ = 7.5 Hz, 3 H), 2.18 (s, 3 H), 2.52 (q, *J*₁ = 7.5 Hz, 2 H), 3.60 (brs, 2 H), 5.65 (s, 1 H), 6.80 (d, *J*₂ = 8.4 Hz, 2 H), 6.81 (s, 2 H), 7.38 (d, *J*₂ = 8.4 Hz, 2H). ¹³C NMR (126 MHz, CDCl₃) δ: 149.4, 139.3, 131.1, 128.6, 126.5 (d, *J* = 3.7 Hz), 124.9 (d, *J* = 270.4 Hz), 123.8, 123.1, 121.9, 119.6 (q, *J* = 32.4 Hz), 113.3, 24.2, 17.8, 13.0. IR (KBr) ν (cm⁻¹): 3385, 2934, 2873, 1110. HRMS (ESI) calcd. for C₁₆H₁₇F₃N₂ [M+H]⁺ *m/z*: 295.1417, found 295.1411.

3,5-Diethyl-*N*'-(4-(trifluoromethyl)phenyl)benzene-1,4-diamine (9f). Yellow oil, 49 mg, yield 16%, ¹H NMR (300 MHz, CDCl₃) δ: 1.26 (t, *J*₁ = 7.5 Hz, 6 H), 2.54 (q, *J*₁ = 7.5 Hz, 4 H), 3.63 (brs, 2 H), 5.69 (s, 1 H), 6.82 (d, *J*₂ = 8.4 Hz, 2 H), 6.84 (s, 2 H), 7.39 (d, *J*₂ = 8.4 Hz, 2 H). ¹³C NMR (126 MHz, CDCl₃) δ: 149.4, 138.7, 131.3, 128.9, 126.6 (q, *J* = 3.5 Hz), 124.9 (q, *J* = 270.3 Hz), 121.7, 119.7 (q, *J* = 33.1 Hz), 113.3, 24.3, 13.0. IR (KBr) ν (cm⁻¹): 3385, 2965, 2874, 1111. HRMS (ESI) calcd. for C₁₇H₁₉F₃N₂ [M+H]⁺ *m/z*: 309.1573, found 309.1572.

4-[(2-Amino-5-methylphenyl)amino]-3,5-dimethylbenzonitrile (15a). Pink crystals, 88 mg, yield 35%, m.p. 133-134 °C, ¹H NMR (300 MHz, CDCl₃) δ: 2.13 (s, 9 H), 3.65 (s, 2 H), 5.02 (s, 1 H), 6.17 (s, 1 H), 6.70 (s, 2 H), 7.36 (m, 2H). ¹³C NMR (75 MHz, CDCl₃) δ: 145.5, 135.4, 132.5, 131.3, 131.2, 129.0, 123.7, 119.6, 119.3, 116.3, 105.4, 20.6, 18.5. IR (KBr) ν (cm⁻¹): 3459, 3365, 2924, 2855, 2220, 1601. HRMS (ESI) calcd. for C₁₆H₁₇N₃ [M+H]⁺ *m/z*: 252.1495, found 252.1502.

4-[(2-Amino-5-ethylphenyl)amino]-3-ethyl-5-methylbenzonitrile (15b). Pink oil, 45 mg, yield 16%, ¹H NMR (300 MHz, CDCl₃) δ: 1.07 (t, *J*₁ = 7.6 Hz, 3H), 1.17 (t, *J*₂ = 7.5 Hz, 3H), 2.08 (s, 3 H), 2.40 (q, *J*₁ = 7.6 Hz, 2H), 2.53 (q, *J*₂ = 7.5 Hz, 2H), 3.64

(s, 2 H), 5.10 (s, 1 H), 6.15 (s, 1 H), 6.68-6.75 (m, 2 H), 7.35 (s, 1 H), 7.39 (s, 1 H). ¹³C NMR (75 MHz, CDCl₃) δ: 144.8, 137.3, 135.8, 135.2, 132.5, 132.1, 131.9, 130.5, 122.1, 119.7, 117.6, 116.4, 105.9, 28.1, 24.4, 18.6, 16.0, 13.8. IR (KBr) ν (cm⁻¹): 3366, 2964, 2917, 2871, 2849, 2221, 1599. HRMS (ESI) calcd. for C₁₈H₂₁N₃ [M+H]⁺ *m/z*: 280.1808, found 280.1814.

Typical procedure for the intercrossing experiments

A solution of *N,N'*-diaryl hydrazine **14a** (35 mg, 0.1 mmol), **14b** (38 mg, 0.1 mmol) [or **7a** (36 mg, 0.1 mmol), **7e** (39 mg, 0.1 mmol)], and conc. HCl (0.15 mL) in 10 mL of 95% ethanol was refluxed for 2 hrs under nitrogen. The reaction mixture was cooled to room temperature, neutralized with solid NaHCO₃, filtered, concentrated. The residue was subjected to the LC-MS analysis.

Typical procedure for the radical trapping experiments

A solution of *N,N'*-diaryl hydrazine **7d** (190 mg, 0.5 mmol) or **14a** (176 mg, 0.5 mmol), TEMPO (78 mg, 0.5 mmol, 2,2,6,6-tetramethyl-1-piperidinyloxy, free radical), and conc. HCl (0.2 mL) in 10 mL of 95% ethanol was refluxed for 2 hrs under nitrogen. The reaction mixture was cooled to room temperature, neutralized with solid NaHCO₃, filtered, concentrated. The residue was purified by flash column chromatography on silica gel to afford **8d** (22% yield) and **9d** (17% yield), respectively, or 41 mg of **15a** as pink crystals in 33% yield.

Acknowledgment

This work was supported in part by The National Basic Research Program of China (No. 2013CB328905), the National Natural Science Foundation of China (Nos. 21372025 and 21172017) and specialized Research Fund for the Doctoral Program of Higher Education, Ministry of Education of China (No. 20110010110011). This paper is also supported by "Chemical Grid Project" of Beijing University of Chemical Technology.

Notes and references

State Key Laboratory of Chemical Resource Engineering, Department of Organic Chemistry, Faculty of Science, Beijing University of Chemical Technology, Beijing 100029, People's Republic of China, Fax/Tel: +86 10 64435565; E-mail: jxxu@mail.buct.edu.cn

[‡]These two authors contributed equally.

[†] Electronic Supplementary Information (ESI) available: Details of rearrangement reactions, copies of ¹H NMR and ¹³C NMR spectra of products, copies of LC-MS diagrams, and computational details. See DOI: 10.1039/b000000x/

- B[1,3]-sigmatropic shift: (a) G. Zweifel, A. Hornig, *Synthesis*, 1973, **11**, 672. (b) K. G. Hancock and J. D. Kramer, *J. Am. Chem. Soc.*, 1973, **95**, 6463. (c) B. M. Miklailov, *Organomet. Chem. Rev., Sect. A*, 1972, **8**, 1. (d) G. W. Kramer and H. C. Brown, *J. Organomet. Chem.*, 1977, **132**, 9. (e) M. Biihl, P. R. Schleyer, M. A. Ibrahim and T. Clark, *J. Am. Chem. Soc.*, 1991, **113**, 2466. (f) U. Henriksen, J. P. Snyder and T. A. Halgren, *J. Org. Chem.*, 1981, **46**, 3767.
- C[1,3]-sigmatropic shift: (a) R. W. Thies, *J. Am. Chem. Soc.*, 1972, **94**, 7074. (b) G. R. Krow and J. Reilly, *J. Am. Chem. Soc.*, 1975, **97**, 3837. (c) J. W. Lown, M. H. Akhtar and W. M. Dadson, *J. Org. Chem.*, 1975, **40**, 3363. (d) R. Fusco and F. Sanniccolo, *Tetrahedron Lett.*, 1976, **17**, 3991. (e) R. W. Thies and E. P. Seitz, *J. Chem. Soc., Chem. Commun.*, 1976, 846. (f) S. Bartlett, R. D. Chambers and N. M. Kelly, *Tetrahedron Lett.*, 1980, **21**, 1891. (g) J. Barluenga, F. Aznar, R. Liz and M. Bayod, *J. Chem. Soc., Chem. Commun.*, 1984, 1427. (h) C. Bleasdale and D. W. Jones, *J. Chem.*

- Soc., Chem. Commun.*, 1985, 1026. (i) M. E. Jung and S. M. Kaas, *Tetrahedron Lett.*, 1989, **30**, 641. (j) D. Desmaele and N. Champion, *Tetrahedron Lett.*, 1992, **33**, 4447. (k) B. Franzus, M. L. Scheinbaum, D. L. Waters and H. B. Bowlin, *J. Am. Chem. Soc.*, 1976, **98**, 1241. (l) K. Seki, W. Kiyokawa, H. Hashimoto, T. Ueyehara, M. Ueno and T. Sato, *Chem. Lett.*, 1996, 1035. (m) F. X. Talamas, D. B. Smith, A. Cervantes, F. Franco, S. T. Cutler, D. G. Loughhead, D. J. Morgans Jr. and R. J. Weikert, *Tetrahedron Lett.*, 1997, **38**, 4725. (n) Y. L. Chen, C. K. Chang and N. C. Chang, *J. Chin. Chem. Soc.*, 1998, **45**, 649. (o) P. Bisel, G. Lauktien, E. Weckert and A. W. Frahm, *Tetrahedron: Asymmetry*, 1998, **9**, 4027. (p) J. D. Bender, P. A. Leber, R. R. Lirio and R. S. Smith, *J. Org. Chem.*, 2000, **65**, 5396. (q) J. E. Baldwin, *Chem. Rev.*, 2003, **103**, 1197. (r) P. Wipf, D. L. Waller and J. T. Reeves, *J. Org. Chem.*, 2005, **70**, 8096. (s) B. O. Ashburn, R. G. Carter and L. N. Zakharov, *J. Org. Chem.*, 2008, **73**, 7305.
- 5 3 Si[1,3]-sigmatropic shift: (a) K. Mach, F. Turecek, H. Antropiusova and V. Hanus, *Organomet.*, 1986, **5**, 1215. (b) M. T. Pereira, M. Pfeffer and M. A. Rotteveel, *J. Organomet. Chem.*, 1989, **375**, 139. (c) M. Takahashi and M. Kira, *J. Am. Chem. Soc.*, 1997, **119**, 1948. (d) M. Takahashi and M. Kira, *J. Am. Chem. Soc.*, 1999, **121**, 8597.
- 20 4 S[1,3]-sigmatropic shift: (a) K. Noerckjaer, A. Senning, *Chem. Ber.*, 1993, **126**, 73. (b) V. Ficeri, P. Kutschy, M. Dzurilla and J. Imrich, *Collect. Czech. Chem. Commun.*, 1994, **59**, 2650. (c) J. Maddaluno, O. Gaonach, A. Marcual, L. Toupet and G. P. Claude, *J. Org. Chem.*, 1996, **61**, 5290.
- 5 P[1,3]-sigmatropic shift: (a) K. Lammertsma, J. T. Hung, P. Chand and G. M. Gray, *J. Org. Chem.*, 1992, **57**, 6557. (b) B. Wang, C. H. Lake and K. Lammertsma, *J. Am. Chem. Soc.*, 1996, **118**, 1690.
- 6 (a) R. B. Woodward, R. Hoffmann, *The Conservation of Orbital Symmetry*; Verlag Chemie: Weinheim, 1970. (b) I. Fleming, *Frontier Orbitals and Organic Chemical Reactions*; Wiley-Interscience: New York, 1976.
- 30 7 S. L. Hou, X. Y. Li and J. X. Xu, *J. Org. Chem.*, 2012, **77**, 10856.
- 8 A. W. Hofmann, *Proc. Roy. Soc. (London)* 1863, **12**, 576.
- 9 R. B. Carlin, R. G. Nelb and R. C. Odioso, *J. Am. Chem. Soc.*, 1951, **73**, 1002.
- 10 A different product ratio (**2**, 85% and **3**, 15%) was reported by Shine and co-workers. See ref. 12f.
- 35 11 (a) M. J. S. Dewar, In *Molecular Rearrangement*, P. de Mayo Ed.; Interscience: New York, 1969; *Vol. 1*, pp 323–343; (b) H. J. Shine, In *Mechanisms of Molecular Migrations*, B. S. Thyagarajan. Ed.; Interscience: New York, 1969; *Vol. 2*, pp 191–247; (c) H. J. Shine, In *Aromatic Rearrangement*, Elsevier: New York, 1967; pp 126–179. (d) R. A. Cox and E. Bunce, In *The Chemistry of the Hydrazo, Azo, and Azoxy Groups*, S. Patai Ed.; Wiley: New York, 1975; pp 775–859. (e) D. V. Banthorpe, R. Bramley and J. A. Thomas, *J. Chem. Soc.*, 1964, 2864. (f) D. V. Banthorpe, *Chem. Rev.* 1970, **70**, 295. (g) G. A. Olah, K. Dunne, D. P. Kelly and Y. K. Mo, *J. Am. Chem. Soc.*, 1972, **94**, 7438. (h) J. D. Cheng and H. J. Shine, *J. Org. Chem.*, 1975, **40**, 703. (i) C. A. Bunton and R. J. Rubin, *J. Am. Chem. Soc.*, 1976, **98**, 4236. (j) A. Zhu-Ohlbach, R. Gleiter, R. Bleiter, H. L. Schmidt and T. Reda, *Eur. J. Org. Chem.*, 1998, **11**, 2409. k) E. Bunce, *Can. J. Chem.*, 2000, **78**, 1251.
- 50 12 (a) H. J. Shine, *J. Phys. Org. Chem.*, 1989, **2**, 491 (review). (b) J. A. Berson, *J. Phys. Org. Chem.*, 2005, **18**, 572.
- 13 (a) H. J. Shine, G. N. Henderson, A. Schmid and P. Cu, *J. Am. Chem. Soc.*, 1977, **99**, 3719. (b) H. J. Shine, H. Zmuda, K. H. Park, H. Kwart, A. G. Horgan, C. Collins and B. E. Maxwell, *J. Am. Chem. Soc.*, 1981, **103**, 955. (c) H. J. Shine, H. Zmuda, K. H. Park, H. Kwart, A. G. Horgan and M. Brechbiel, *J. Am. Chem. Soc.*, 1982, **104**, 2501. (d) H. J. Shine, K. H. Part, M. L. Brownawell and J. San Filippo, Jr. *J. Am. Chem. Soc.*, 1984, **106**, 7007. (e) W. Subotkowski, L. Kupczyk-Subotkowska and H. J. Shine, *J. Am. Chem. Soc.*, 1993, **115**, 5073.
- 60 14 (a) H. J. Shine, E. Gruszecka, W. Subotkowski, M. Brownawell and J. San Filippo, Jr. *J. Am. Chem. Soc.*, 1985, **107**, 3218. (b) H. J. Shine, L. Kupczyk-Subotkowska and W. Subotkowski, *J. Am. Chem. Soc.*, 1985, **107**, 6674; 1987, **109**, 1286. (c) L. Kupczyk-Subotkowski, H. J. Shine, W. Subotkowski and J. Zygmunt, *Gazz. Chim. Ital.* 1987, **117**, 513.
- 65 15 (a) H. J. Shine, H. Zmuda, H. Kwart, A. G. Horgan and M. Brechbiel, *J. Am. Chem. Soc.*, 1982, **104**, 5181. (b) E. S. Ree and H. J. Shine, *J. Am. Chem. Soc.*, 1986, **108**, 1000; 1987, **109**, 5052. (c) E. S. Rhee and H. J. Shine, *J. Org. Chem.*, 1987, **52**, 5633. (d) H. J. Shine, In *Isotopes in Organic Chemistry*, E. Bunce and W. H. Saunders, Jr., Eds.; Elsevier: Amsterdam, 1992; Vol. 8, Chapter 1.
- 70 16 S. Yamabe, H. Nakata and S. Yamazaki, *Org. Biomol. Chem.*, 2009, **7**, 4631.
- 17 G. Ghigo, S. Osella, A. Maranzana and G. Tonachini, *Eur. J. Org. Chem.*, 2011, 2326.
- 18 M. J. Smith and J. March, In *Advanced Organic Chemistry*, John Wiley & Sons, Hoboken, New Jersey, 2007; chapter 18–36, pp.1678–1681.
- 75 19 K. Y. Kim, J. T. Shin, K. S. Lee and C. G. Cho, *Tetrahedron Lett.*, 2004, **45**, 117.
- 20 (a) J. Jacobson, *Justus Liebigs Ann. Chem.*, 1922, **428**, 76. (b) C. K. Ingold and H. W. Kidd, *J. Chem. Soc.*, 1933, 984.
- 80 21 M. J. Frisch, et al. Gaussian 09, Revision B.01; Gaussian, Inc.: Wallingford, CT, 2010.
- 22 (a) A. D. Becke, *J. Chem. Phys.*, 1993, **98**, 5648. (b) C. Lee, W. Yang and R. G. Parr, *Phys. Rev. B*, 1988, **37**, 785.
- 23 (a) V. Barone and M. Cossi, *J. Phys. Chem. A*, 1998, **102**, 1995. (b) M. Cossi, N. Rega, G. Scalmani and V. Barone, *J. Comput. Chem.*, 2003, **24**, 669. (c) Y. Takano and K. N. Houk, *J. Chem. Theory Comput.*, 2005, **1**, 70.
- 85 24 For recent examples of distortion/interaction analysis, see: (a) D. H. Ess and K. N. Houk, *J. Am. Chem. Soc.*, 2007, **129**, 10646. (b) D. H. Ess and K. N. Houk, *J. Am. Chem. Soc.*, 2008, **130**, 10187. (c) P. H.-Y. Cheong, R. S. Paton, S. M. Bronner, G.-Y. Im, N. K. Garg and K. N. Houk, *J. Am. Chem. Soc.*, 2010, **132**, 1267. (d) P. Liu, P. McCarren, P. H. Cheong, T. F. Jamison and K. N. Houk, *J. Am. Chem. Soc.*, 2010, **132**, 2050. (e) Y. Lan and K. N. Houk, *J. Am. Chem. Soc.*, 2010, **132**, 17921 and references cited therein.
- 90 25 Although slight carbon KIEs were observed in the rate-limiting step in the rearrangements, the phenomena have been found in the concerted 1,3-dipolar cycloaddition of *N*, α -diphenylnitrene and styrene with a carbon KIE ranging from 1.012 to 1.068 depending on which carbon atom was labelled (Ref. 26), and the concerted [2 + 2] cycloaddition of diphenylketene and styrene with a carbon KIE in the range of 1.0055–1.08 (Ref. 27).
- 100 26 B. M. Benjamin and C. J. Collins, *J. Am. Chem. Soc.*, 1973, **95**, 6145.
- 27 C. J. Collins, B. M. Benjamin and G. W. Kabalka, *J. Am. Chem. Soc.*, 1978, **100**, 2570.
- 28 For reviews, see (a) S.E. Scheppele, *Chem. Rev.* **1972**, **72**, 511. (b) A. Maccoll, *Annu. Rep. Prog. Chem., Sect. A. Inorg. and Phys. Chem.* **1974**, **71**, 77. For examples, see (c) J. Bron and J. B. Stothers, *Can. J. Chem.*, **1968**, **46**, 1435. (d) J. Bron and J. B. Stothers, *Can. J. Chem.*, **1969**, **47**, 2506.
- 105 110